

¹⁹W. Schmidt and U. Strohhbusch, Nucl. Phys. **A159**, 104 (1970).

²⁰J. W. Watson, private communication.

²¹K. Bethge, C. M. Fou, and R. W. Zurmühle, Nucl. Phys. **A123**, 521 (1969).

²²D. J. Johnson and M. A. Waggoner, Phys. Rev. C **2**,

41 (1970).

²³H. G. Benson and B. H. Flowers, Nucl. Phys. **A126**, 305 (1969).

²⁴V. V. Davidow and L. M. Pavlichenkov, Phys. Letters **29B**, 551 (1969).

PHYSICAL REVIEW C

VOLUME 5, NUMBER 3

MARCH 1972

Pionic X-Ray Yields and $2p$ -Level Widths in ${}^6\text{Li}$, ${}^9\text{Be}$, ${}^{12}\text{C}$, and ${}^{16}\text{O}^\dagger$

W. W. Sapp, Jr.,* M. Eckhause, G. H. Miller,‡ and R. E. Welsh

College of William and Mary, Williamsburg, Virginia 23185

(Received 7 September 1971)

We have measured the intensities of $2p$ - $1s$ pionic x-ray transitions in ${}^6\text{Li}$, ${}^9\text{Be}$, ${}^{12}\text{C}$, and ${}^{16}\text{O}$ using an absolute-efficiency technique. A pion-cascade calculation which was constrained to reproduce the observed yields predicted population probabilities for the mesonic levels and gave values for the strong-interaction level widths. The $2p$ -level broadenings are 0.015 ± 0.005 eV for ${}^6\text{Li}$, 0.16 ± 0.03 eV for ${}^9\text{Be}$, 2.1 ± 0.6 eV for ${}^{12}\text{C}$, and 12 ± 4 eV for ${}^{16}\text{O}$. Comparisons are made with results obtained by others and with predictions based upon a semiphenomenological optical potential. Empirical capture schedules for π^- in ${}^6\text{Li}$ and ${}^{12}\text{C}$ are also presented.

I. INTRODUCTION

The yield, or intensity, of the $2p$ - $1s$ pionic atomic transition, defined as the number of $K\alpha$ x rays emitted per stopped pion, can be used to deduce the nuclear-absorption rate for a pion in the $2p$ state.¹ Ericson and Ericson² have described the absorptive interaction in terms of an imaginary part of a semiphenomenological optical potential. A recent analysis by Krell and Ericson³ has suggested that either this optical potential does not satisfactorily describe $2p$ -state absorption for all elements or that a systematic uncertainty exists in one or both of the experimental methods used to determine the absorption rates. In particular, measurements in elements with $Z \leq 11$ were in substantial disagreement with predictions based on measurements in higher- Z elements. We wish to report here the first measurement of the $2p$ - $1s$ pionic transition yield in ${}^6\text{Li}$ in addition to new measurements for ${}^9\text{Be}$, ${}^{12}\text{C}$, and ${}^{16}\text{O}$. The yield in ${}^9\text{Be}$ is in excellent agreement with a recently reported value⁴ from CERN, but is in disagreement with another measurement by Berezin *et al.*⁵ Previously published^{4,6} yields in ${}^{12}\text{C}$ and ${}^{16}\text{O}$ (as H_2O) which were based on comparisons between muonic and pionic x-ray spectra are substantially larger than those obtained in this investigation.

The results of the present work compare favorably with predictions based on an optical potential whose constant parameters have been independent-

ly determined⁷ from selected pionic x-ray data. A secondary purpose of this investigation was to determine the capture schedule for π^- in ${}^6\text{Li}$, for which no previous measurements exist. This capture schedule is of particular interest to those engaged in a theoretical comparison of radiative pion capture and muon capture in this element.⁸ The capture schedule for ${}^{12}\text{C}$ is also presented because of apparent disagreements in the literature^{9,10} on the interpretation of existing yield data.

II. EXPERIMENTAL TECHNIQUE AND DATA ANALYSIS

The data were obtained in two experiments using a 190-MeV/c negative-pion beam of the NASA Space Radiation Effects Laboratory (SREL) synchrocyclotron. Standard scintillation-counter coincidence techniques were used to obtain a π -stop signal. A 1600-channel analyzer sorted and stored pulses from a Si(Li) or Ge(Li) detector when a coincidence existed between the π -stop signal and the detector signal. The timing window for this coincidence was 320 nsec wide and was typically about 3 times the full width at 0.1 maximum of the timing peak. Other features of the experiment were the following:

(1) Absolute muonic x-ray yields were also measured to investigate systematic errors which might have arisen either in the experiments or in the data analysis. The muonic K series is particularly use-

ful for this purpose, since it is generally accepted that the total series yield is very nearly unity in all elements,¹¹ with the probable exception of Li. The pionic and muonic L -series x-ray yields were measured also for Mg and Ti, since these x rays bracket in energy the K series of C and O. The yields obtained for these "reference" lines are generally in good agreement with earlier work and with the predictions of cascade calculations.¹²

(2) The detector used with each of the elements was chosen on the basis of efficiency requirements. For the ${}^6\text{Li}$ and ${}^9\text{Be}$ targets an $80\text{-mm}^2 \times 3\text{-mm}$ Si(Li) detector was used; for the K -series transitions in ${}^{12}\text{C}$ and ${}^{16}\text{O}$ and the L -series transitions in Mg and Ti, a $770\text{-mm}^2 \times 40\text{-mm}$ coaxial Ge(Li) detector was employed. The ${}^{12}\text{C}$ and Mg x rays were also studied using a high-resolution $350\text{-mm}^2 \times 5\text{-mm}$ planar Ge(Li) detector.

(3) Before and/or after each mesonic x-ray data accumulation, absolute detector efficiencies were determined *in situ* using calibrated sources.¹³

(4) All targets except H_2O consisted of one or more thin plates which facilitated measurement of x-ray absorption coefficients to be used in target self-absorption corrections. For all targets except H_2O the total thickness along the beam axis was less than 2.0 g/cm^2 ; for the H_2O target it was 2.46 g/cm^2 .

(5) As shown in Fig. 1, the plane of the targets

was perpendicular to the target-detector axis and at an angle of 45° with respect to the beam axis. The detectors were out of the direct beam on the low-momentum side and were carefully shielded.

Peaks in the mesonic x-ray spectra were analyzed primarily to determine the number of x rays corresponding to the transitions of interest and the uncertainties to be assigned to those numbers. The identification and subtraction of contaminant peaks were accorded special attention. Muonic x-ray contamination in the pionic x-ray spectra was systematically subtracted using the relative intensities obtained from separate μ -beam data. Figure 2(a) shows "raw" data from a data run in the pion beam; in Fig. 2(b) the muonic x-ray spectrum has been subtracted. Contaminations from nuclear γ rays (following pion capture) and x rays from mesons stopping in any material other than the target were subtracted using different *ad hoc* techniques. At least two independent methods were used to determine the background and as a rule gave consistent results. Discrepancies never exceeded 2.0 standard deviations and were generally less than 1.5. In these cases the spectra were reexamined, possible causes of the discrepancy established, and a final result selected with an assigned uncertainty larger than either of the independent uncertainties.

The total number of pions stopping in the target

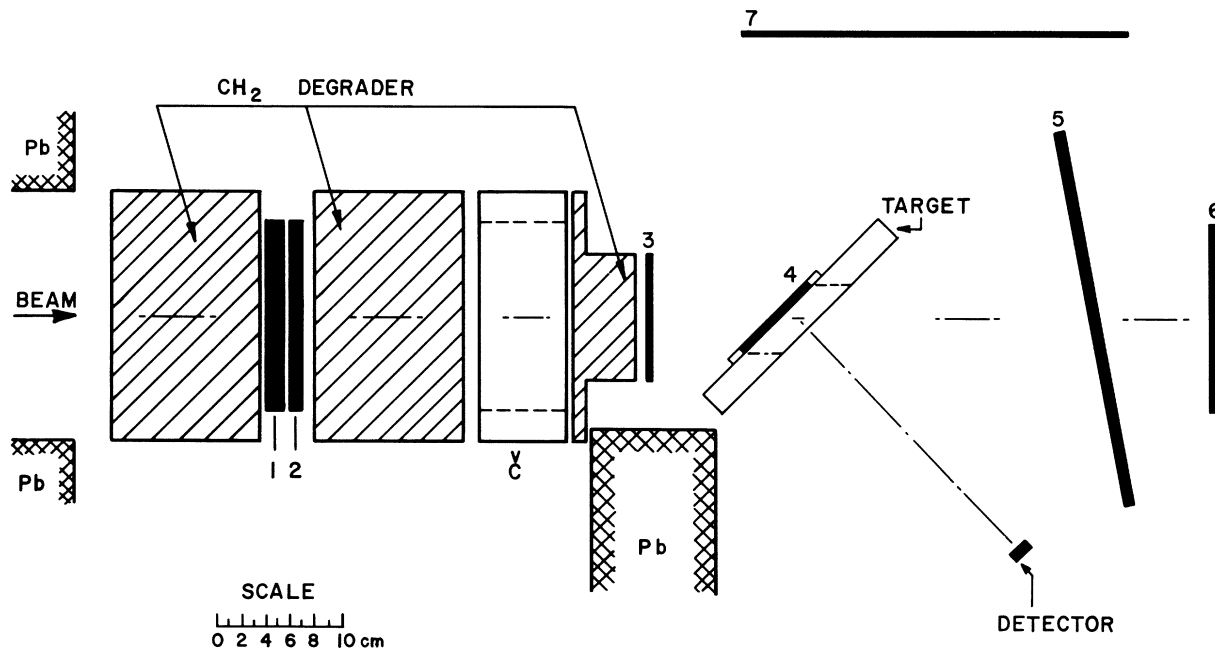


FIG. 1. Counter geometry. The degrader upstream of counter 1 was used only during the muonic x-ray runs. The particle-stopping signature was $12\bar{C}345$, C being a water-filled Čerenkov counter sensitive to high-energy electrons; all other counters were plastic scintillants. Counter 6 was used to monitor the efficiency of 5 and counter 7 was used to record beam particles outscattered by the target.

during an x-ray run was taken to be the scaled number of stop signatures corrected for veto-counter efficiency, outscattering, events which gave the proper signature but which occurred in nontarget materials, and muon contamination in the pion beam. According to range-curve analyses this contamination was about 6 and 9% on the two runs, respectively, while investigation of muonic x-ray peaks in the pionic x-ray spectra indicated contamination ranging from 2.5 to 5% in the first run and 2.5 to 7% in the second run. The generally large uncertainties associated with these numbers do not entirely exclude possible systematic differences between targets. Because of this difficulty the most probable value for the contamination was selected, and it was assumed the same for all targets in the run. These uncertainties in

the muon contamination contributed less than 2% to the uncertainties in the final values for the absolute yields. The experimental absolute yields are given in Table I, column two, where they are compared with previously published results.

III. LEVEL POPULATIONS AND ABSORPTION BROADENING

If the atomic processes are sufficiently well understood to allow an accurate prediction of the population probability of the pionic $2p$ state then the measured $2p-1s$ x-ray yields provide a direct measure of the nuclear-capture broadening, $\Gamma_{2p}(\text{cap})$. The capture broadening is related to the yield, population probability, and competing electromagnetic transition rates by:

$$\Gamma_{2p}(\text{cap}) = \frac{P_{2p}\Gamma_{2p}(\text{rad})}{Y_{2p-1s}(\text{rad})} - [\Gamma_{2p}(\text{rad}) + \Gamma_{2p}(\text{Auger})],$$

where $\Gamma_{2p}(\text{rad})$ and $\Gamma_{2p}(\text{Auger})$ are the calculated partial widths for the $2p-1s$ radiative and Auger transitions, respectively, and Y_{2p-1s} is the yield of the pionic $2p-1s$ transition.¹⁴ The population probability P_{2p} is deduced from either atomic-cascade calculations,¹⁵ or observations of other x-ray transitions, or both. A detailed discussion of the determination of the population probabilities is given in Ref. 12. The results of these calculations are presented in Table I, column three. Column four contains the values for the strong-interaction broadening, $\Gamma_{2p}(\text{cap})$, deduced using the above equation.

The cascade calculation, constrained to reproduce the observed x-ray yields, predicts the popu-

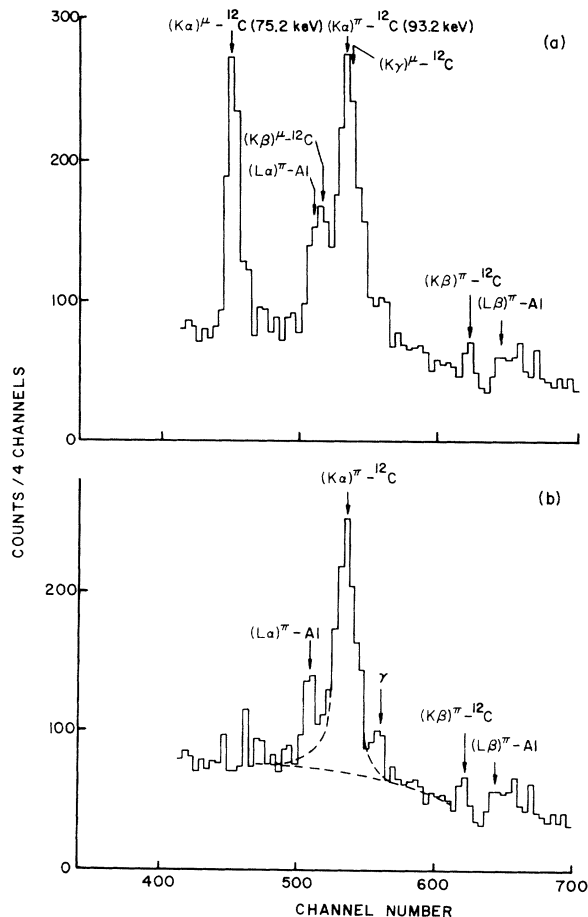


FIG. 2. (a) ^{12}C pionic x-ray spectrum. (b) ^{12}C pionic x-ray spectrum with $K\alpha$, $K\beta$, and $K\gamma$ muonic x-ray peaks subtracted. Additional evidence for the contaminant peaks from aluminum was obtained from other spectra. The combined counts in four adjacent channels have been plotted. The dashed lines represent fits to the $K\alpha$ pionic x-ray peak and the random background.

TABLE I. Measured pionic x-ray yields, deduced population probabilities, and absorption broadening of the $2p$ levels in ^6Li , Be, C, and O.

Element	Yield ($2p-1s$)	P_{2p}	$\Gamma_{2p}(\text{cap})$ (eV)
^6Li	0.26 ± 0.03	0.68 ± 0.04	0.015 ± 0.004
^9Be	0.10 ± 0.01	0.64 ± 0.03	0.16 ± 0.03
	0.105 ± 0.014^a	0.67 ± 0.07^b	0.16 ± 0.03^b
	0.19 ± 0.06^c	$\leq 0.55^c$	0.053 ± 0.013^c
^{12}C	0.035 ± 0.010	0.67 ± 0.04	2.6 ± 0.9
	0.075 ± 0.020^b	0.62 ± 0.06^b	1.02 ± 0.29
	0.082 ± 0.006^d		
^{16}O	0.020 ± 0.005	0.57 ± 0.04	12 ± 4
	0.049 ± 0.007^e	0.57 ± 0.06^b	4.7 ± 0.8^b

^a Reference 4.

^b Reference 1.

^c D. P. Earty, Ph.D. thesis, University of Chicago, 1969 (unpublished); and Ref. 5.

^d A. R. Kunselman, University of California (Berkeley) Report No. UCRL-18654, 1969 (unpublished).

^e Reference 6.

lation probability and the capture probability for all pionic states in the atom. The products of these two probabilities constitute the "capture schedule" for the mesonic atom. The capture schedules for the lower levels in pionic ${}^6\text{Li}$ and ${}^{12}\text{C}$ are given in Table II.^{16, 17}

IV. COMPARISON WITH THEORY

We compare our results with predictions obtained using a semiphenomenological optical potential whose form was derived by Ericson and Ericson.² This potential, which is based on a multiple scattering theory, has, in principle, no adjustable parameters¹⁸ and predicts the absolute pion-absorption rate as well as the dependence of this rate upon Z and other properties of the nucleus. It should be realized, however, that the relative absorption rates for different nuclei are model-independent, to a first approximation. Thus agreement between theory and experiment upon general Z (or A) dependence of the rates is no indication of the success of the present model. It is the ability of the theory to predict absolute rates and model-dependent phenomena, such as isospin effects, which must be examined.

It should also be remembered that predictions of this model depend on a knowledge of the nuclear-matter distribution. In particular, absorption of the pion from $2p$ states is sensitive to the distribution of nucleons near the nuclear surface.³

The optical potential of Ref. 3 contains constant parameters which may be constrained such that the potential reproduces experimentally observed pionic x-ray energies and widths. The comparison of these "best-fit" parameters with those predicted from π -nucleon scattering lengths and pion-production cross sections constitutes a test of hypotheses upon which these predictions are based. The "best-fit" parameters may also be used to predict the energies and widths of x-ray lines which have not yet been measured.

The technique employed in the present analysis was to use optical-potential parameters obtained from a best fit to selected pionic x-ray data to predict $2p$ -level widths in low- Z elements.¹⁹ The best-fit analysis was limited to direct linewidth measurements of monoisotopic, nondeformed nuclei whose charge distributions had been determined experimentally. The requirement that the linewidth be measured directly rather than by the indirect yield method insured that the resulting best-fit parameters were not biased by possible systematic errors in the indirect method. The restriction of isotopic purity of the target and a good knowledge of the nuclear-charge distribution were imposed because of the aforementioned sensitivity of the model's predictions to the distribution of nuclear matter. 38 targets fulfilled the monoisotopic and spherical-nuclei requirements, and direct width measurements of either the $2p$, $3d$, or $4f$ level had been made in 16 of the 38 nuclei. The methods used to determine the nucleon densities and the general calculational techniques are described by Anderson, Jenkins, and Powers.⁷

In Fig. 3 we have plotted "reduced widths" (essentially division of width by Z^6) versus mass number A in order to remove most of the model-independent behavior. The solid curve is based on the "best-fit" parameters⁷ of the optical-model potential noted above. The solid circles are the results of direct width measurements and were used in the determination of the "best-fit" parameters. The solid triangle is a revision¹ of an earlier direct measurement of the $2p$ -level width in ${}^{31}\text{P}$. This revision, because it represents such a small fraction of the total amount of data used, should have a very small effect on the best fit given by the solid curve.²⁰ All open symbols indicate the results of indirect (yield) determinations of the widths and were not used in obtaining the "best-fit" parameters. The solid curve for $A < 31$ then constitutes *predicted* values of the widths to which

TABLE II. Nuclear-capture schedules for pions in ${}^6\text{Li}$ and ${}^{12}\text{C}$. Listed are the number of pions captured from each state *per* atomically captured pion.

$n \setminus l$	${}^6\text{Li}$		${}^{12}\text{C}$	
	0	1	0	1
5	0.006 ± 0.004	0.005 ± 0.0005	0.0035 ± 0.0015	0.038 ± 0.007
4	0.016 ± 0.006	0.035 ± 0.001	0.0025 ± 0.0015	0.082 ± 0.008
3	0.022 ± 0.007	0.130 ± 0.006	0.0015 ± 0.0008	0.145 ± 0.002
2	0.019 ± 0.005	0.430 ± 0.075	0.003 ± 0.001	0.63 ± 0.05
1	0.335 ± 0.065		0.06 ± 0.02	
Total s -state capture:	0.40 ± 0.09		0.08 ± 0.03	
Total p -state capture:		0.60 ± 0.09		0.92 ± 0.03
Total d -state capture:		$\sim 1 \times 10^{-5}$		$\sim 7 \times 10^{-4}$

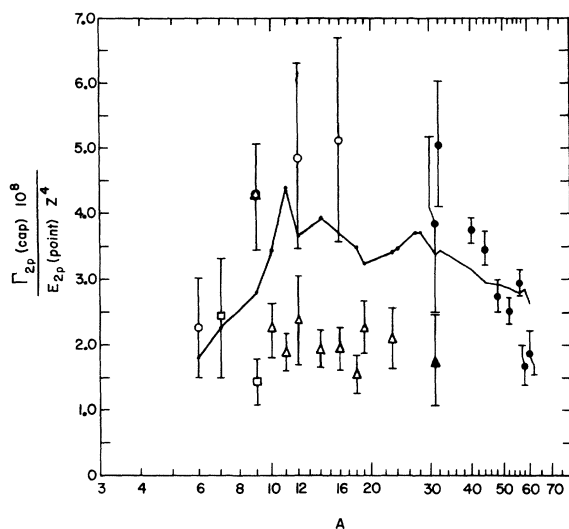


FIG. 3. Reduced $2p$ -level widths versus mass number A . The solid curve is the best fit to selected data using an optical-model potential (see text). Level widths deduced from yield measurements (indicated by the open symbols) were not used to obtain the best fit; the curve for $A < 31$ may then be thought of as a theoretical prediction. The open circles are the results of the present experiment, the open triangles are from Ref. 1, and the open squares are from Ref. 5.

these indirect measurements can be compared. The open circles are the results of the present experiment, the open triangles are from results reported by CERN,¹ and the open squares are the results of Berezin *et al.*⁵

V. SUMMARY

The results of the present experiment compare favorably with theoretical predictions based on the best-fit parameters of Anderson, Jenkins, and Powers⁷ and suggest that the optical potential discussed in Sec. I may satisfactorily describe $2p$ absorption for a wide range of elements. More quantitative conclusions must await substantial reductions in the uncertainties of the measured widths and improved knowledge of the nuclear-matter distribution in low- Z elements.

There is a large discrepancy between the results obtained here and those of the CERN group^{4,6} for the elements ^{12}C and ^{16}O . There is, however, excellent agreement between these results for ^9Be and those of the CERN group,^{4,6} but not those reported by Berezin *et al.*⁵ The primary source of the discrepancies is in the different values obtained for experimental absolute yields. Level populations obtained using cascade calculations are in general agreement. Absolute muonic x-ray yields measured in this experiment were in good agreement with predictions based on cascade calculations¹² and with earlier work, and served as an independent check of the experimental method.

VI. ACKNOWLEDGMENTS

We are indebted to Professor D. Anderson for helpful discussions and for performing the phenomenological fit to the data. We thank Professor J. Hüfner for providing us with his muon-cascade program. We also wish to thank Dr. R. T. Siegel and the staff of SREL for their support.

†Work supported in part by the National Aeronautics and Space Administration and by the National Science Foundation.

*J. E. Zollinger Fellow 1969–1970. Present address: Brookhaven National Laboratory, Upton, New York 11973.

‡Gulf Oil Corporation Graduate Fellow 1970–1971.

¹G. Backenstoss, in *Proceedings of the Third International Conference on High Energy Physics and Nuclear Structure*, edited by S. Devons (Plenum, New York, 1970), p. 469. References to earlier work are given.

²M. Ericson and T. E. O. Ericson, *Ann. Phys. (N.Y.)* **36**, 323 (1966).

³M. Krell and T. E. O. Ericson, *Nucl. Phys.* **B11**, 521 (1969).

⁴H. Koch *et al.*, *Phys. Letters* **29B**, 140 (1969).

⁵S. Berezin, G. Burlison, D. Earty, A. Roberts, and T. O. White, *Nucl. Phys.* **B16**, 389 (1970).

⁶H. Koch *et al.*, *Phys. Letters* **28B**, 380 (1968).

⁷D. K. Anderson, D. A. Jenkins, and R. J. Powers, *Phys. Rev. Letters* **24**, 71 (1970). There is good general agreement between the results of this theoretical work and that of Ref. 3.

⁸See J. Delorme, *Nucl. Phys.* **B19**, 573 (1970); P. Pascual and A. Fujii, *Nuovo Cimento* **65**, 411 (1970). Both papers contain references to earlier work.

⁹H. Hilscher *et al.*, *Nucl. Phys.* **A158**, 584 (1970), especially their note p. 592.

¹⁰J. A. Bistirlich *et al.*, *Phys. Rev. Letters* **25**, 689 (1970).

¹¹M. B. Stearns, G. Culligan, B. Sherwood, and V. L. Telegdi, *Phys. Rev.* **184**, 22 (1969).

¹²W. W. Sapp, College of William and Mary Report No. WM-21, 1970 (unpublished).

¹³Single solid γ sources, International Atomic Energy Agency, Vienna, Austria. Knowledge of the shapes of the Ge(Li) detectors' efficiency curves was improved by employing an uncalibrated ^{133}Ba source which emits several γ rays whose relative intensities have been previously determined [D. P. Donnelly *et al.*, *Phys. Rev.* **173**, 1192 (1968)].

¹⁴Exact pionic $2p$ - $1s$ radiative rates for ^9Be , ^{12}C , and ^{16}O given in Ref. 1 were used in the present analysis. For ^6Li , hydrogenic wave functions were used in conjunction with the experimental $2p$ - $1s$ transition energy to obtain the radiative rate.

¹⁵We are greatly indebted to J. Hüfner who kindly provided us with a copy of his muon-cascade program, which served as the basis for all of our cascade calculations.

¹⁶The capture schedule for ${}^6\text{Li}$ was obtained using capture broadening of 150 eV and 2×10^{-8} eV for the $1s$ and $3d$ states, respectively. For ${}^{12}\text{C}$, the corresponding values were 3250 eV and 1.5×10^{-5} eV, respectively. [See R. J. Harris *et al.*, Phys. Rev. Letters **20**, 505 (1968).] The results given in Table II are insensitive to uncertainties in these assumed values.

¹⁷H. Hilscher *et al.* (Ref. 9) apparently assumed that mesons are captured from only the $2p$ or $1s$ state, whereas

Bistirlich *et al.* (Ref. 10) apparently assumed that the $1s$ state population is equal to the $2p$ - $1s$ x-ray yield. Both of these assumptions are incorrect, as indicated in Tables I and II.

¹⁸Conforming with the authors of Ref. 4 we have assumed the *ad hoc* nucleon-nucleon correlation parameter of the potential to be unity.

¹⁹We are grateful to D. K. Anderson, D. A. Jenkins, and R. J. Powers for the calculated predictions and for their permission to present these results.

²⁰D. K. Anderson, private communication.

Tensor Correlations in Nuclear Matter: Three-Body Effects*

M. L. Ristig

Institut für Theoretische Physik, Universität zu Köln, 5 Köln 41, Germany

and

W. J. Ter Louw and J. W. Clark†

Compton Laboratory of Physics, Washington University, St. Louis, Missouri 63130

(Received 4 November 1971)

The Jastrow method has been extended to the treatment of tensor forces by the incorporation of suitable spin and isospin dependence into the correlation operators. Here the three-body contributions to the factor-cluster expansion of the energy expectation value are evaluated for nuclear matter, supplementing the evaluation of the one- and two-body contributions already reported in the first paper of this series. Complete numerical results are presented for three semirealistic hard-core potentials containing differing mixtures of central and tensor components. The three-body corrections result in a distinct improvement of the saturation behavior of the approximate energy per particle. Nevertheless, these calculations should be regarded as still exploratory rather than final in the sense that the most intelligent (i.e., a suitably restricted) choice of radial dependence has not yet been determined for the correlation functions.

I. INTRODUCTION

It is commonplace to remark on the complexity of the nucleon-nucleon force: its strong repulsion at short distances, its state dependence (i.e., its dependence on spin, isospin, and total angular momentum), and especially its strong tensor component. These complexities have received careful attention in the well-established Brueckner-Bethe-Goldstone (BBG) theory^{1,2} of the ground-state energy of nuclear matter. The literature offers numerical investigations of the two-hole-line diagrams (as defined in BBG theory) for a variety of realistic and semirealistic nuclear potentials.³ There are also calculations of the three-hole-line diagrams⁴ based on the Bethe-Faddeev scheme.⁵ However, among the studies of this type, only those of Dahlblom⁶ and Day⁷ (who also considers four-hole-line diagrams) include the effect of the tensor component in an adequate man-

ner, and not just in terms of an "equivalent" central potential.

In order to study the effects of tensor correlations in nuclear matter – or finite nuclei – we have recently proposed an approach exploiting the original Jastrow idea, in the enlarged context of the method of correlated basis functions.⁸ We have begun with a relatively simple (and surely limited) realization of the general scheme. It is our immediate purpose to make explicit the merits and deficiencies of this simple picture. Afterwards we can still proceed, if necessary, to more complicated structures; i.e., we can incorporate additional physical information (e.g., impose conservation of certain "sum rules" in each cluster order,⁹ examine higher-order perturbative corrections with respect to the non-orthogonal basis of correlated wave functions,¹⁰ change to a different ansatz for the Jastrow correlation factor, invoke a more highly summed cluster expansion,¹¹ etc.).